Transverse excitations of ultracold matter waves upon propagation past abrupt waveguide changes

M. Koehler, M. W. J. Bromley,* and B. D. Esry[†]

Department of Physics, Kansas State University, Manhattan, Kansas 66506, USA

(Received 14 October 2004; published 3 August 2005)

The propagation of ultracold atomic gases through abruptly changing waveguide potentials is examined in the limit of noninteracting atoms. Time-independent scattering calculations of microstructured waveguides with discontinuous changes in the transverse harmonic binding potentials are used to mimic waveguide perturbations and imperfections. Three basic configurations are examined: steplike, barrierlike, and well-like with waves incident in the ground mode. At low energies, the spectra rapidly depart from single moded, with significant transmission and reflection of excited modes. The high-energy limit sees 100% transmission, with the distribution of the transmitted modes determined simply by the overlap of the mode wave functions and interference.

PACS number(s): 03.75.Be, 03.75.Kk, 03.65.Nk

I. INTRODUCTION

The manipulation of ultracold matter waves can now, somewhat routinely, be performed above microchip or magnetized surfaces [1,2]. In such experiments, the quantum nature of the dilute atomic gases dominates over the classical, enabling precision matter wave control [3].

One of the key requirements in using an "atom chip" to perform atom optics is the ability to transport atoms from one atom optical component to another. Here, we present calculations of wave propagation through waveguides with idealized perturbations consisting of sudden changes to the transverse confining potential. An increase (decrease) in the tranverse confining potential results in a decrease (increase) in the kinetic energy along the direction of wave propagation, providing effective step potentials along the waveguide.

The present study was motivated in three ways. First, recent experiments have demonstrated a significant fragmentation of a Bose-Einstein condensate (BEC) in a waveguide located close to the surfaces [4,5], attributed, at least in part, to imperfections created during the wire fabrication processes [6–10]. Secondly, to further understand some of the limitations to designing atom optics devices that are based on variations of the waveguide potentials, for example, the smoothly varying wide-narrow-wide wire geometry has been proposed as a quantum-point-contact type device for atoms [11]. Thirdly, the literature has been lacking a multimode analysis of many of the simplest waveguide geometries, as it has been experimentally shown that introducing a perturbation in a waveguide can result in the transverse excitation of a BEC [4].

To characterize the impact of transverse discontinuities, here we explore the Schrödinger wave mechanics of waveguides with steplike, barrierlike, and well-like potentials along the direction of propagation. There have already been some theoretical investigations using time-dependent calculations of wave propagation through smooth potentials such as a bottleneck (step-up) and a smooth termination (extreme step-down) in the limit of noninteracting atoms [12,13], while nonlinear (atom-atom) effects in the bottleneck-type geometry have also been examined [14,15]. The advantages in using abrupt potentials whilst neglecting atom-atom interactions is that simple time-independent calculations can be used to characterize the transmission and reflection probabilities. Under these conditions, we have previously investigated a circular bend [16], which consists of an abrupt transition from the lead waveguides into the bend and at low-energies behaves like a potential well.

Our multimode analysis, restricted as it is to the linear regime, provides a baseline for comparison of BEC propagation through quasi-one-dimensional (1-D) waveguides including the transverse degrees of freedom. For example, previous time-independent studies have investigated non-linear wave propagation through shallow-well, step and Gaussian shaped 1D potentials [17–20]. Such simple waveguide potentials could be generated by modifying the transverse confinement, where knowledge of the transverse excitation probabilities, in the abrupt and linear limits, should be useful.

For ground mode matter waves propagating at low energies through the various perturbations, the present results show that the spectra rapidly depart from single-moded, with significant transmission and reflection of excited modes. The high-energy limit sees 100% transmission, and we present a simple model to determine the distribution of the transmitted modes that combines the overlap of the mode wave functions with the multipath interference of the modes.

II. DETAILS OF THE POTENTIALS

There are a number of atom chip wire configurations that can create waveguides [2,21], but we follow the theoretical ansatz adopted in Refs. [16,22]. That is, we assume that the waveguides consist of an idealized trapping potential that is quadratic near the minimum and operate at low matter-wave densities such that atom-atom interactions can be neglected. Furthermore, so that the waveguide potentials reduce to an

———————
*Electronic address: bromley@phys.ksu.edu

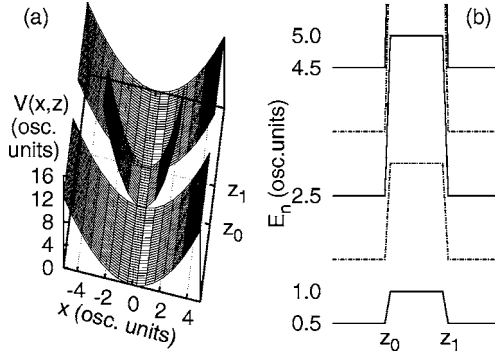[†]Electronic address: esry@phys.ksu.edu

FIG. 1. (a) Potential energy surface of a barrierlike waveguide with $\omega_a=1$ and $\omega_b=2$ and barrier length $l=z_1-z_0$. (b) Energy levels of the leads and barrier transverse SHO potential along z. The solid lines at z_0 and z_1 should be vertical, but instead are drawn on an angle to highlight the lead-barrier-lead transition. The dot-dashed lines correspond to the parity-forbidden levels (assuming an even incoming mode). All the energies and coordinates are given in terms of oscillator units for the leads.

TABLE I. Conversion of oscillator units to S.I. units for ^{23}Na atoms trapped by a transverse oscillator frequency $\omega=2\pi\times 97$ Hz. The energy and velocity thresholds for each even SHO mode are given in oscillator units. Given in S.I. units are the temperature, velocity, and wavelength corresponding to each modes threshold.

n	E (osc.)	v_z (osc.)	E_k (μK)	v_z (mm s^{-1})	λ (μm)
0	0.5	0	0	0	∞
2	2.5	2	77.41	2.595	6.69
4	4.5	$2\sqrt{2}$	154.8	3.669	4.73
8	8.5	4	309.6	5.189	3.34
16	16.5	$4\sqrt{2}$	619.3	7.338	2.36
32	32.5	8	1239	10.38	1.67

effective 2D problem, the waveguides are assumed to be created by multiple wire configurations with abrupt changes in the spacing between the wires, such that the height and transverse position of the potential minima remains constant along the waveguide. The out-of-plane quantum number is then a conserved quantity.

We consider simple harmonic oscillator (SHO) confining potentials, which, for barrierlike or well-like effective potentials, are given by

$$V(x,z)=\begin{cases}\frac{1}{2}m\omega_a^2x^2, & z\leq z_0,\\ \frac{1}{2}m\omega_b^2x^2, & z_0\leq z\leq z_1,\\ \frac{1}{2}m\omega_a^2x^2, & z\geq z_1.\end{cases}\qquad(1)$$

The barrierlike potential has $\omega_b>\omega_a$; the well-like potential has $\omega_a>\omega_b$. The steplike potential consists of only one change in frequency.

Oscillator units are used throughout this paper, where energies are in units of $\hbar\omega$, while lengths are given in units of $\beta=\sqrt{\hbar/m\omega}$. An example barrierlike potential is shown in Fig. 1(a), where the reference frequency is $\omega_a=1$, while $\omega_b=2$. The corresponding energy levels of Eq. (1) are shown in Fig. 1(b). These energy levels behave as effective potentials for the longitudinal motion since we expand the total wave function in each region on the transverse oscillator states. In this model, all coupling between modes occurs through the matching between regions. The potentials in Eq. (1) are symmetric in x so that parity in x is conserved, simplifying the present analysis and discussion considerably [the dot-dashed lines in Fig. 1(b) are not coupled to the solid lines]. In experiments, imperfections would as likely be off-center, resulting in populating of all modes (as was possible in our previous study of the circular bend [16]). The fundamental physics, however, remains much the same, so we chose to adopt parity-conserving perturbations with the incoming waves restricted to the ground (even) oscillator mode.

To compare the calculations presented throughout this paper with experiment, Table I shows some typical S.I. values

for ^{23}Na atoms trapped in a waveguide with a transverse oscillator frequency of $\omega=2\pi\times 97$ Hz as per the experiment of Leanhardt *et al.* [4]. This combination gives $\beta\approx 2.128$ μm. Table I gives the longitudinal velocity, temperature, and wavelength of the atomic cloud as they relate to the thresholds of propagation for each even transverse mode of the waveguide. A similar table was given in Ref. [22] for ^{87}Rb atoms.

III. DETAILS OF THE CALCULATIONS

To perform the time-independent scattering calculations we initially adopted the transfer matrix method [23], although most of the calculations reported in this paper use the interface matching method [16,23]. The two methods are similar, however, and since the transfer matrix approach facilitates the discussion of our results, we outline it here. The extension of the transfer matrix method from one dimension to include transverse degrees of freedom is somewhat trivial [24,25], so only a short summary is given here as it applies to a barrier/well-like geometry of length $(z_1-z_0)=l$.

First, the time-independent wave function is expanded on transverse SHO states, $\varphi_n(x)$ for frequencies ω_a, and $\chi_m(x)$ for ω_b:

$$\Psi_{\mathrm{I}}(x,z)=\sum_n \varphi_n(x)[a_ne^{ik_n(z-z_0)}+b_ne^{-ik_n(z-z_0)}]z\leq z_0,$$

$$\Psi_{\mathrm{II}}(x,z)=\sum_m \chi_m(x)[c_me^{i\kappa_m(z-z_0)}+d_me^{-i\kappa_m(z-z_0)}]z_0\leq z\leq z_1,$$

$$\Psi_{\mathrm{III}}(x,z)=\sum_n \varphi_n(x)[g_ne^{ik_n(z-z_1)}+h_ne^{-ik_n(z-z_1)}]z_1\leq z. \quad(2)$$

where the momenta are $k_n=\sqrt{2E-\omega_a(2n+1)}$ and $\kappa_m=\sqrt{2E-\omega_b(2m+1)}$. Matching the wave functions and their first derivatives across each interface and then projecting out the modes gives the following sets of equations:

$$\begin{pmatrix}\vec{a}\\\vec{b}\end{pmatrix}=\begin{pmatrix}A^{11}&A^{12}\\A^{21}&A^{22}\end{pmatrix}\begin{pmatrix}\vec{c}\\\vec{d}\end{pmatrix}\text{ and }\begin{pmatrix}\vec{c}\\\vec{d}\end{pmatrix}=\begin{pmatrix}B^{11}&B^{12}\\B^{21}&B^{22}\end{pmatrix}\begin{pmatrix}\vec{g}\\\vec{h}\end{pmatrix}.$$

$$(3)$$

The matrix elements of each submatrix are

$$A_{nm}^{11} = A_{nm}^{22} = \frac{1}{2}\left(1 + \frac{\kappa_m}{k_n}\right)O_{nm},$$

$$A_{nm}^{12} = A_{nm}^{21} = \frac{1}{2}\left(1 - \frac{\kappa_m}{k_n}\right)O_{nm},$$

$$B_{mn}^{11} = e^{-2i\kappa_m l}B_{mn}^{22} = \frac{1}{2}\left(1 + \frac{\kappa_m}{k_n}\right)e^{-i\kappa_m l}O_{nm},$$

$$B_{mn}^{12} = e^{-2i\kappa_m l}B_{mn}^{21} = \frac{1}{2}\left(1 - \frac{\kappa_m}{k_n}\right)e^{-i\kappa_m l}O_{nm}, \tag{4}$$

using the notation $O_{nm} = \int \varphi_n(x)\chi_m(x)dx$. While generating functions are known for the overlaps of SHO functions with different frequencies [26,27] (such overlaps are also found in calculations of transitions between molecular vibrational modes [28]), we performed the transverse integrations numerically using a B-spline basis.

The scattering solution is obtained by constructing the transfer matrix $Q = AB$, which relates one lead's coefficients, $\vec{a}$ and $\vec{b}$, to the other's, $\vec{g}$ and $\vec{h}$. Given that the wave is restricted to incoming from $z < z_0$ in the ground mode ($a_0 = 1$, $a_{n_i>0} = 0$, and $\vec{h} = \vec{0}$), the linear equation $\vec{a} = Q^{11}\vec{g}$ is solved, and then $\vec{b} = Q^{21}\vec{g}$. The transmission and reflection probabilities for each mode are then given by

$$T_{n_f} = \frac{|g_{n_f}|^2 k_{n_f}}{|a_0|^2 k_0} \text{ and } R_{n_f} = \frac{|b_{n_f}|^2 k_{n_f}}{|a_0|^2 k_0}. \tag{5}$$

The multimode transfer matrix method eliminates the need to find intermediate coefficients (i.e., $\vec{c}$ and $\vec{d}$) and is easier to implement than the interface matching method. Our single-mode transfer matrix program was validated by reproducing the single-mode calculations of electron propagation through a linear array of 1D potentials [29]. The results from the multimode transfer matrix method were then validated against an independent 2D interface matching program [16].

Transfer matrix convergence issues were mentioned in passing by Wu *et al.* [24], where the method was applied to a system of multiple circular bends. In the end, however, the calculations shown in Ref. [24] were performed using multiple interface matching. No such issues were noted in the multichannel transfer matrix calculations of Pereyra and Castillo [25,30], where delta potentials provide minimal mode-coupling at the interfaces. Our experience mirrors both of these studies. Our calculations found that the multimode transfer matrix approach suffers from inaccuracy only when it is necessary to include a large number of closed modes in a calculation [31].

Both methods are employed in this paper. The calculations for the steplike potentials use the transfer matrix method, while interface matching is used for the barrierlike and the well-like potentials. The transfer matrix method does achieve convergence for the step-like geometries (i.e., for a single interface, simply $Q = A$). The interface matching method was otherwise used in this paper for all the barrier/well-like potentials and was able to include enough closed

modes to ensure near machine-precision results. For the most extreme interface matching calculations of barrierlike potentials, up to $N = 96$ modes were required to obtain unitarity, $1 - \Sigma_f(T_{n_f} + R_{n_f})$, to better than 10^{-10}.

IV. RESULTS

The multimoded transmission and reflection probabilities for three basic geometries are given in this section: the steplike potential, the barrierlike potential and the well-like potential. Before presenting these calculations, it is instructive to discuss how the interface overlaps O_{0m} scale with frequency.

A. Interface overlaps

The O_{0m} dependence on the frequency ratio ω_b/ω_a is discussed here since it strongly influences the amount of mode excitation caused by the different geometries. Using the orthonormality of the SHO eigenstates, along with the recursion relations of the Hermite polynomials, it can be shown that the overlap integrals of the $\omega_a = 1$ ground mode with the ω_b even modes reduce to the particularly simple form:

$$O_{0m} = \sqrt{\frac{2\sqrt{\omega_b}(m-1)!!}{(\omega_b+1)m!!}}\left(\frac{\omega_b-1}{\omega_b+1}\right)^{m/2}, \tag{6}$$

for all $m = 0, 2, 4, 6\ldots$. Due to symmetry, $O_{0m} = 0$ for $m = 1, 3, 5\ldots$. Equation (6) was also obtained by Aslangul [27].

The dependence of the first three overlaps ($m = 0, 2, 4$) on frequency is shown in Fig. 2(a). At $\omega_b = 1$, there is a perfect waveguide match, and we must have $O_{00} = 1$ and $O_{0m} = 0$ for $m > 0$. As ω_b increases, O_{00} monotonically decreases towards zero. At the same time, the overlap with each excited mode increases and reaches a maximum when the characteristic
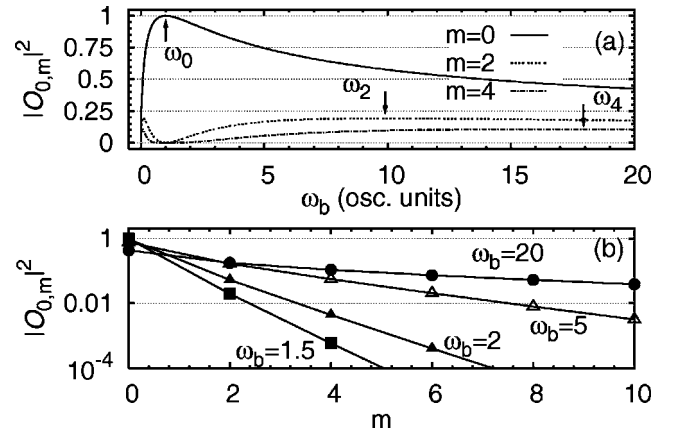
FIG. 2. SHO wave function overlaps $|O_{0m}|^2$ between the ground mode with fixed frequency $\omega_a = 1$, and another mode with variable frequency ω_b. (a) Shows the $m = 0, 2, 4$ modes as a function of ω_b. The arrows labeled by ω_m indicate the maxima. (b) Shows the overlaps as a function of m for four frequencies: $\omega_b = 1.5$ (squares), $\omega_b = 2$ (filled triangle), $\omega_b = 5$ (hollow triangle), and $\omega_b = 20$ (circles). The lines between dots in (b) are added to guide the eye. The frequencies shown in both (a) and (b) are given in oscillator units relative to ω_a.
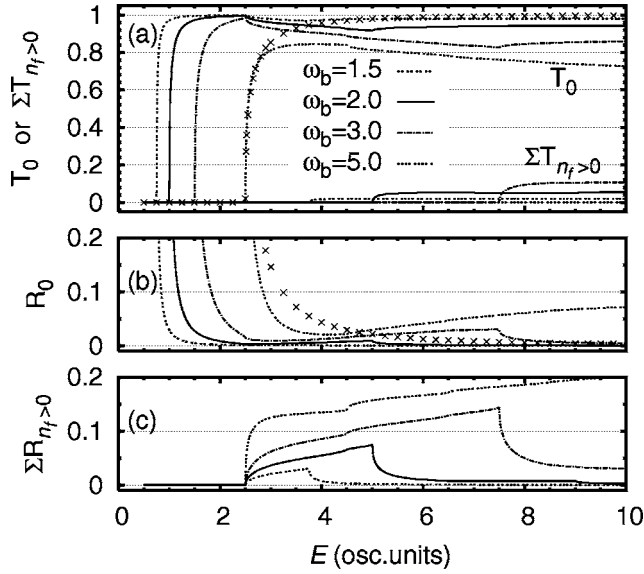
FIG. 3. Multimoded scattering probabilities of steplike potentials which consist of a single abrupt change in the transverse confinement potential from $\omega_a=1$ to $\omega_b=1.5$, 2, 3, and 5. The incoming waves are in the ground state $n_i=0$. (a) Shows T_0 and $\Sigma T_{n_f>0}$, the transmission probabilities into the ground mode and the sum of the transmission probabilities into the excited modes, respectively. (b) Gives R_0, the reflection probabilities into the ground mode, while (c) gives $\Sigma R_{n_f>0}$, the sum of the reflection probabilities into the excited modes. The total energy E is given in oscillator units relative to ω_a. The crosses in (a) and (b) are the analytic transmission and reflection probabilities for a 1D step potential for the case of $\omega_b=5$ (i.e., of height $V_0=|2.5-0.5|$ with a background potential $V=0.5$ added to correct the reflection ground mode threshold).

equation, $\omega_b^2-2(2m+1)\omega_b+1=0$, is satisfied. As a function of frequency, these maxima occur at $\omega_m=(2m+1)+\sqrt{(2m+1)^2-1}$, which, for $m=2$, is $\omega_2=9.8989$ and for $m=4$, is $\omega_4=17.944$. Comparing the width ($\sqrt{\langle x^2\rangle}$) of the SHO functions at these frequencies against the ground mode's reveals that $\sqrt{\langle x_m^2(\omega_m)\rangle}\approx\sqrt{1/4}=\sqrt{\langle x_0^2\rangle}/2$. This connection, while natural, is not particularly illuminating and is not pursued here any further. Past the maxima, the overlaps slowly decrease as $\omega_b^{-1/4}$ to zero. Due to symmetry of the ratio ω_b/ω_a, a second maxima of $|O_{0m}|^2$ also exists at $1/\omega_m$.

The slow decay of the overlaps with the higher modes can be seen in Fig. 2(b). This implies that, even at low energies, many closed modes must be included in the following calculations to achieve computational convergence.

B. Steplike waveguide potential

The transmission and reflection probabilities, T_{n_f} and R_{n_f}, of ground mode plane waves traversing four steplike waveguides are shown in Fig. 3. At incident energies below the lowest reflection threshold ($E<2.5$, the lowest excited mode energy), the system behaves like the familiar 1D step potential. Ground state transmission, T_0, remains the dominant channel across the range of energies shown in Fig. 3(a) (for the range of ω_b examined here), although excited mode transmission can also be seen in Fig. 3(a) as each mode
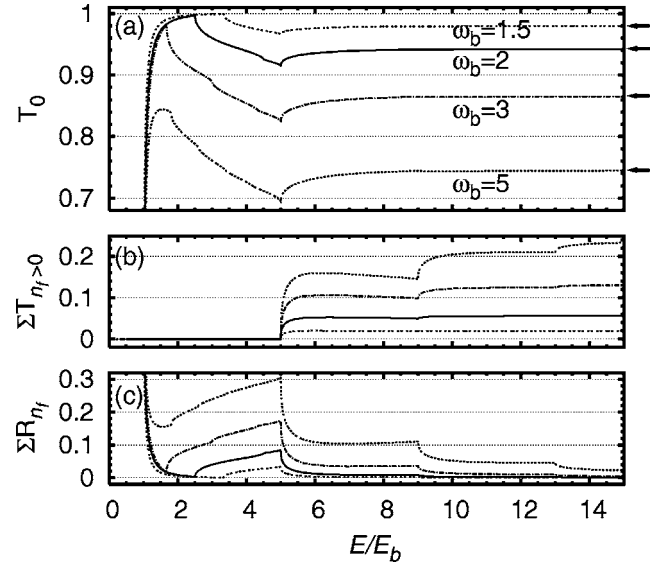

FIG. 4. The scattering probabilities of the same four steplike potentials as Fig. 3 ($\omega_b=1.5$, 2, 3, and 5) plotted here as a function of E/E_b, where $E_b=\omega_b/2$. For each waveguide, (a) shows the transmission probabilities of the ground mode, (b) the sum of the excited mode transmission probabilities $\Sigma T_{n_f>0}$, and (c) the total reflection probabilities ΣR_{n_f}. The arrows at $E/E_b=15$ correspond to the $|O_{00}|^2$ interface overlaps.

opens. Significant reflection is seen into the ground $n_f=0$ mode in Fig. 3(b), which rapidly drops off from threshold. As each reflection threshold opens, the reflection into the excited modes $n_f>0$, seen in Fig. 3(c), first increases then is seen to experience an overall decrease. All of which are consistent with the Wigner threshold laws for multichannel systems [32].

For incidence in the ground channel, the total transmission approaches 100% in the high-energy limit. In this limit the transmission probability is given simply by

$$T_{n_f}(E\rightarrow\infty)=|O_{0n_f}|^2, \qquad (7)$$

with the SHO overlaps of Eq. (6). Such projections were introduced as part of the waveguide calculations of Jääskeläinen and Stenholm [12,33], in which the transmission excitation probabilities generated by both bottleneck and split-potential waveguides were briefly discussed as the potentials tended towards abrupt. Similar multimode projections have also been theoretically examined during expansion of a BEC from a microtrap into a waveguide [15], with an emphasis on the effects of atom-atom interactions.

Equation (7) can be seen as the high-energy limit of the matrix elements of A, given by Eq. (4). At energies high compared to the step height, the momenta of the lowest few modes are approximately the same on both sides of the step, $\kappa_{n_f}\approx k_0$. Given that the overlaps limit the number of modes involved, the matrix elements that dominate the $Q=A$ transfer matrix are then $A_{0,n_f}^{11}=A_{0,n_f}^{22}\approx O_{0n_f}$, while $A_{0,n_f}^{12}=A_{0,n_f}^{21}\approx0$. For an incoming wave in the ground mode with $a_0=1$, $a_{n_i>0}=0$, and $\vec{d}=0$, then the outgoing waves have $c_{n_f}\approx O_{0n_f}$ while $\vec{b}=0$.
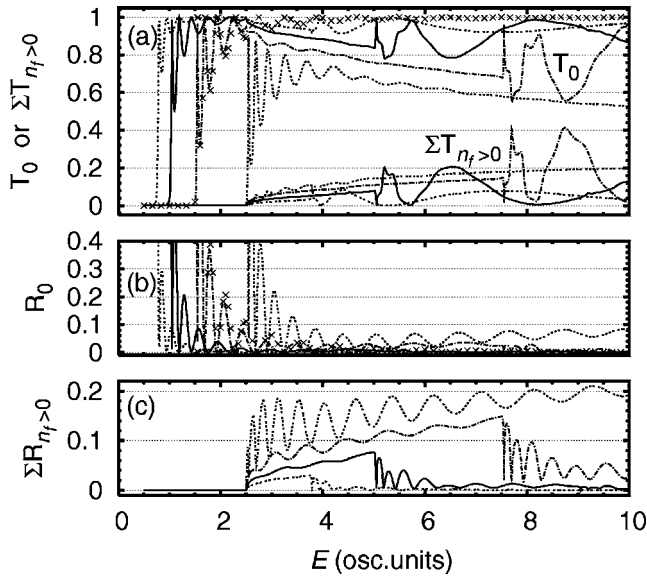
FIG. 5. Multimoded scattering probabilities of four barrierlike potentials with $\omega_b = 1.5$, 2, 3, and 5 for a fixed length $l = 10$ as a function of E (in oscillator units relative to ω_a). The legend for the different frequencies is the same as Figs. 3 and 4. The organization of the probabilities is also the same as Fig. 3. The crosses in (a) and (b) are the analytic transmission and reflection probabilities for a 1D barrier potential for the case of $\omega_b = 3$ (i.e., of height $V_0 = |1.5 - 0.5|$ with a background potential $V = 0.5$).

To clearly show this limit, the results of Fig. 3 are replotted in Fig. 4 on an energy axis scaled by ω_b instead of ω_a so that the transmission modes for each waveguide open at the same scaled energy. At high energies, the transmission probabilities shown in Fig. 4(a) increase towards asymptotes of $T_0(E \to \infty) = |O_{00}|^2$, in agreement with Eq. (7). For the four different waveguides shown here, the limits are $T_0(E \to \infty) = 0.979796$, 0.942809, 0.866026, and 0.745356. Figures 4(b) and 4(c) show that at the onset of each transmitted mode (i.e., at $E/E_b = 5$, 9, etc.) the transmission probability into that mode increases, taking flux from reflection. The mismatch in mode wave functions for $\omega_b = 5$, for example, is particularly severe, with $T_{n_f = 0,2,4,6}(E \to \infty) = 0.745356$, 0.165635, 0.055212, and 0.020449 [see Fig. 2(b)]. In this case, these four transmission modes must be open before the high-energy limit [$\Sigma T_{n_f} = 1$, as per Eq. (7)] is reached to within 2%.

Whether the wave is incident from the left or the right, these results apply. The ground mode transmission $T_0(E)$ is *absolutely identical* as a function of total energy E for both the waveguide constriction (i.e., step-up from $\omega_a = 1$ to $\omega_b > 1$), and the waveguide expansion (i.e., step-down from $\omega_a > 1$ to $\omega_b = 1$) These results also hold for the familiar 1D step potential, and, although we do not show it here, the transmission and reflection mode mixing conspire to ensure this is also the case in the multichannel system. The mode mixing as a function of E is different for either geometry, however, since for the step-up case there can be many reflection modes open at the lowest transmission threshold, $E = E_b$, while for the step-down, there can be many transmission modes open at $E = E_b$. At high energies, neither of the
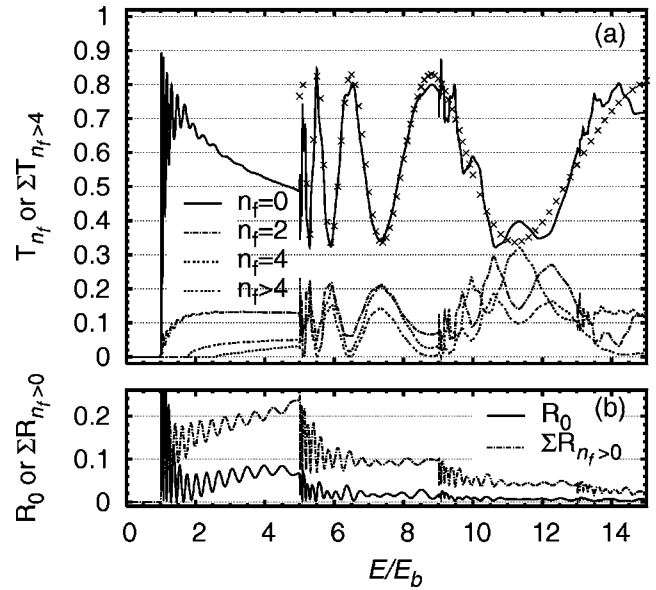

FIG. 6. The scattering probabilities of the $\omega_b = 5$, $l = 10$, barrierlike potential seen in Fig. 5 plotted here as a function of E/E_b where $E_b = 2.5$. (a) Shows the individual transmission probabilities of the $n_f = 0, 2, 4$ modes alongside the sum of the transmission probabilities for the $n_f > 4$ modes. (b) Shows the ground-mode reflection probabilities as well as the sum of the excited mode reflection probabilities. The crosses in (a) correspond to the $T_0(E \to \infty)$ two-mode interference model of Eq. (8). The first peak of T_0 reaches nearly up to 1, which is not shown due to the limited energy resolution of the figure.

step geometries generates reflection, and for incidence in the ground mode the limits from Eq. (7) apply.

C. Barrierlike waveguide potential

To demonstrate the characteristics of a single barrierlike potential, we consider the case shown in Fig. 1, for a fixed length l and frequencies that change from $\omega_a = 1$ to $\omega_b > \omega_a$ and back to $\omega_a = 1$. We also present the high-energy characteristics for scattering from this potential.

The transmission and reflection probabilities for four waveguide constrictions $\omega_b = 1.5$, 2, 3, 5 and length $l = 10$ are shown in Fig. 5. Resonances appear in all of the spectra at low energies due to the wavelength matching condition $n\lambda/2 \approx l$. The 1D analytic results for $\omega_b = 3$ in Fig. 5(a) highlight the transmission resonances as the result of low-energy ground-mode propagation over the barrier. As soon as the $\omega_a = 1$, $n = 2$ mode opens at $E = 2.5$, however, multichannel physics takes over ($n = 1$ is not allowed due to symmetry). Above $E = 2.5$, there is significant excited mode transmission [Fig. 5(a)], while the amount of reflection into the ground mode [Fig. 5(b)] and the excited modes [Fig. 5(c)] is significant across the energy range.

To observe the high-energy limit, the results for the $\omega_b = 5$ barrier of Fig. 5 were extended to higher energies, and are shown in Fig. 6 with the energy scaled by $E_b = 2.5$. Figure 6(b) shows that while there is more structure in the reflection probabilities than for the steplike potential in Fig. 4(c), the total amount of reflection still tends towards zero as more

barrier modes become open at $E/E_b = 5, 9, 13, \ldots$.

To compare these values with experiment, consider ^{23}Na atoms in a waveguide with frequency $2\pi \times 97$ Hz [4]. A barrier of length $l=10$ corresponds to a constriction 21.28 μm long under these conditions, a dimension well within the capabilities of current atom chip manufacturing techniques.

While only three excited barrier modes are open at $E/E_b = 15$ for all the barriers shown in Fig. 6, there are many more lead modes that are open at this energy. For the extreme $\omega_b = 5$ barrier ($E_b = 2.5$) shown in Fig. 6, the $n=0, 2, 4, 6$ barrier modes become open at $E/E_b = 1, 5, 9, 13$. For the ^{23}Na $2\pi \times 97$ Hz experiment these correspond in S.I. units to $v_z = 2.595, 6.355, 8.605, 10.378$ (mm s^{-1}). In particular, Table I shows that the $n=6$, $\omega_b = 5$ barrier mode opens at the same threshold as the $n=32$, $\omega_a = 1$ lead mode.

To obtain an expression analogous to Eq. (7), we must take into account the fact that the transmitted waves going through a barrier experience at least two interface projections as in Eq. (7). The phases accumulated while propagating the length l of the barrier must also be included in such a prescription, which suggests that at high energies (relative to the barrier height)

$$T_0(E \to \infty) = \left| \sum_m e^{i(\kappa_m - \kappa_0)l} O_{0m} O_{m0} \right|^2, \tag{8}$$

where m is only summed over the propagating barrier modes. The crosses shown in Fig. 6(a) demonstrate that the two-mode version of this model does a remarkable job in describing the transmission probability above the $m=2$ barrier threshold (at $E/E_b = 5$). Depending on the phase differences, the modes that are excited at the first interface can be converted back to the ground mode by the second interface. We also noted this behavior in circular waveguide bends [16], where the amount of excitation could be suppressed by changing the angle swept out by the bend to the point where the accumulated phase difference between the $n=0$ and $n=1$ modes was a multiple of π. A similar design consideration could perhaps be useful for atom optics devices such as the quantum point contacts [11], where any unavoidable—yet unwanted—mode excitations could be minimized by varying the length between the changes in waveguide potentials.

D. Well-like waveguide potential

The transmission and reflection probabilities for well-like waveguides due to a potential bulge ($\omega_a > \omega_b$) are the focus in this last section. The scattering behavior for a well is complicated by the presence of bound states which translate into the presence of Feshbach resonances in a multichannel problem. Much of the resonance physics seen here has been extensively discussed as part of our studies of the circular waveguide bend [16,34]. The propagation thresholds in a bend lie slightly lower than the connecting leads [35,36], resulting in very weakly bound states and energetically narrow resonances. The present well-like waveguides can provide extreme differences between the lead and bulge energy thresholds, and thus the possibility of multiple narrow resonances located below the thresholds.
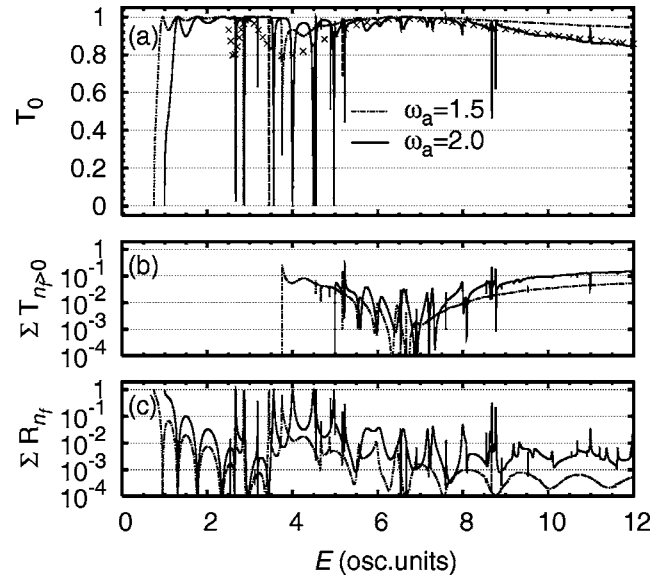

FIG. 7. Multimoded scattering probabilities of two well-like potentials with $\omega_a = 1.5$ and 2 for a fixed length $l=10$ as a function of E (in oscillator units relative to ω_b). The organization of the probabilities is the same as Fig. 4. The crosses in (a) correspond to the $T_0(E \to \infty)$ two-mode interference model of Eq. (8) for $\omega_a = 2$.

Two bulges are considered here, the first from $\omega_a = 1.5$ to $\omega_b = 1$ and back to $\omega_a = 1.5$, and the second with $\omega_a = 2$ to $\omega_b = 1$ and back to $\omega_a = 2$. In both cases, we choose $\omega_b = 1$ to be the reference oscillator frequency, to simplify the comparison with the barriers in the previous section. The transmission and reflection probabilities of both of these potentials with well length $l=10$ are shown in Fig. 7.

Multiple 100% reflection resonances exist at energies below the first excited lead mode energy, i.e., below $E=3.75$ for $\omega_a = 1.5$ and $E=5$ for $\omega_a = 2$. As was noted in our circular bend studies [16], the reflection resonances below the second excited mode (i.e., below $E=6.75$ for $\omega_a = 1.5$, and at $E=9$ for $\omega_a = 2$) do not result in complete reflection due to the reduced coupling between the ground and second excited mode and due to the existence of alternate pathways to reflection.

The high-energy transmission probability asymptotes for the well-like potential are again given by Eq. (8), although the energy of the first excited mode within the well means that the two-mode model starts at $E=2.5$ (in other words, at a lower energy than for the equivalent barrierlike potential). The two-mode model is shown in Fig. 7(a) for the $\omega_a = 2$ well, and is seen to be a bad approximation near the $E=2.5$ threshold due to the significant reflection there. The two-mode model generally provides a reasonable approximation at higher energies once the total reflection probability has dropped below the total excited mode transmission probability, and also when the many narrow reflection resonances no longer play a role.

Waveguides with more extreme discontinuities such as $\omega_a = 3$ and 5 were also explored. They exhibit so many resonances across the range of energies shown in Fig. 7, however, that the transmission and reflection probabilities essentially become a dense series of closely spaced vertical spikes.

At energies above the second excited mode threshold (E =4.5), there are not so many resonances, although there remains significant reflection probability. As an example, the ω_a=5, l=10, well-like waveguide has a total reflection probability at E=37.5 (E/E_a=15) that has only dropped down to about 0.2. This reflection probability can be compared with the ω_b=5, l=10 barrierlike geometry in Fig. 6(b) at E =37.5 (E/E_b=15), where the total reflection probability was only about 0.02. In other words, reflections play a far more dominant role for the well-like potentials than the barrierlike.

V. SUMMARY

Using time-independent solutions of the Schrödinger equation, we have explored the propagation of dilute, ultracold atomic gases through abruptly changing waveguide potentials. Previous studies have discussed the conditions for "adiabatic" waveguide propagation through microstructures (e.g., Refs. [11–13,37]). In contrast, the interest here was on the consequences of sudden potential variations for mode excitation with a view towards modelling waveguide imperfections, examining the effects of using abrupt potentials in atom optical devices, and simply to explore the behavior of some simple geometries.

Three idealized geometries with changes in the transverse guiding potential have been the focus of study: steplike, barrierlike, and well-like. The low-energy behavior of all the geometries departed from single-moded, with the exception of the mildest perturbations at energies below the lowest excitation threshold. Significant generation of both transmission and reflection excited modes was caused by the mismatch of the modes at the interfaces between the waveguide sections. The strong coupling to excited modes is due to the significant overlap of the ground SHO function of one frequency with the excited SHO functions with a different frequency. Certainly, care should be taken during wire fabrication of atom optical elements to ensure that any deliberate (or not) changes in a waveguides transverse frequency are not abrupt.

High-energy wave propagation through abrupt potentials amounts to 100% wave transmission via projections across each interface, along with multimode interference. The present SHO-based waveguides behave somewhat differently than the hard-walled models for ballistic electron propagation through waveguides with a wide-narrow junction (see Ref. [38], and the references thereafter that cite it). In that case an impedance mismatch occurs, where there is always some amount of reflection at high energies due to the fact that the narrow guide modes can never represent the wide guide modes over the whole width of the lead. Although, to the best of our knowledge, calculations for such electron waveguides have not discussed high-energy/abrupt potential transmission and reflection limits.

A further condition was suggested for high-energy transmission through microstructures with multiple interfaces to account for the interference between modes. It was shown that a simple two-mode model can give a reasonable approximation to the amount of ground mode transmission, and provides an additional consideration for the design of "atomchip" waveguides to control single-moded wavetransmission through potentials that generate multimoded excitations.

[1] E. A. Hinds and I. G. Hughes, J. Phys. D **32**, R119 (1999).

[2] R. Folman, P. Krüger, J. Schmiedmayer, J. Denschlag, and C. Henkel, Adv. At., Mol., Opt. Phys. **48**, 263 (2002).

[3] K. Bongs and K. Sengstock, Rep. Prog. Phys. **67**, 907 (2004).

[4] A. E. Leanhardt, A. P. Chikkatur, D. Kielpinski, Y. Shin, T. L. Gustavson, W. Ketterle, and D. E. Pritchard, Phys. Rev. Lett. **89**, 040401 (2002).

[5] J. Fortágh, H. Ott, S. Kraft, A. Günther, and C. Zimmermann, Phys. Rev. A **66**, 041604(R) (2002).

[6] S. Kraft, A. Günther, H. Ott, D. Wharam, C. Zimmermann, and J. Fortágh, J. Phys. B **35**, L469 (2002).

[7] A. E. Leanhardt, Y. Shin, A. P. Chikkatur, D. Kielpinski, W. Ketterle, and D. E. Pritchard, Phys. Rev. Lett. **90**, 100404 (2003).

[8] D. W. Wang, M. D. Lukin, and E. Demler, Phys. Rev. Lett. **92**, 076802 (2004).

[9] C. J. Vale, B. Upcroft, M. J. Davis, N. R. Heckenberg, and H. Rubinsztein-Dunlop, J. Phys. B **37**, 2959 (2004).

[10] T. Schumm, J. Esteve, C. Figl, J. Trebbla, C. Aussibal, H. Nguyen, D. Mailly, I. Bouchoule, C. I. Westbrook, and A. Aspect, Eur. Phys. J. D **32**, 171 (2005).

[11] J. H. Thywissen, R. M. Westervelt, and M. Prentiss, Phys. Rev. Lett. **83**, 3762 (1999).

[12] M. Jääskeläinen and S. Stenholm, Phys. Rev. A **66**, 023608 (2002).

[13] M. Jääskeläinen and S. Stenholm, Phys. Rev. A **66**, 053605 (2002).

[14] T. Lahaye, P. Cren, C. Roos, and D. Guéry-Odelin, Commun. Nonlin. Sci. Numer. Simul. **8**, 315 (2003).

[15] J. A. Stickney and A. A. Zozulya, Phys. Rev. A **65**, 053612 (2002).

[16] M. W. J. Bromley and B. D. Esry, Phys. Rev. A **68**, 043609 (2003).

[17] P. Leboeuf and N. Pavloff, Phys. Rev. A **64**, 033602 (2001).

[18] P. Leboeuf, N. Pavloff, and S. Sinha, Phys. Rev. A **68**, 063608 (2003).

[19] N. Pavloff, Phys. Rev. A **66**, 013610 (2002).

[20] B. T. Seaman, L. D. Carr, and M. J. Holland, Phys. Rev. A **71**, 033609 (2005).

[21] J. H. Thywissen, M. Olshanii, G. Zabow, M. Drndić, K. S. Johnson, R. M. Westervelt, and M. Prentiss, Eur. Phys. J. D **7**, 361 (1999).

[22] M. W. J. Bromley and B. D. Esry, Phys. Rev. A **69**, 053620 (2004).

[23] E. Merzbacher, *Quantum Mechanics* (Wiley, New York, 1970).

[24] H. Wu and D. W. L. Sprung, Phys. Rev. B **47**, 1500 (1993).

[25] P. Pereyra and E. Castillo, Phys. Rev. B **65**, 205120 (2002).

[26] D. T. Birtwistle, J. Phys. A **10**, 677 (1977).

[27] C. Aslangul, Am. J. Phys. **63**, 1021 (1995).

[28] C. Manneback, Physica (Amsterdam) **17**, 1001 (1951).

[29] H. Wu, D. W. L. Sprung, J. Martorell, and S. Klarsfeld, Phys. Rev. B **44**, 6351 (1991).

[30] P. Pereyra, Phys. Rev. Lett. **80**, 2677 (1998).

[31] M. W. J. Bromley, M. Koehler, and B. D. Esry (unpublished).

[32] U. Fano and A. R. P. Rau, *Atomic Collisions and Spectra* (Academic Press, Orlando, FL, 1986).

[33] M. Jääskeläinen, Ph.D. thesis, Royal Institute of Technology, Stockholm, 2003.

[34] M. W. J. Bromley and B. D. Esry, Phys. Rev. A **70**, 013605 (2004).

[35] P. Exner and P. Seba, J. Math. Phys. **30**, 2574 (1989).

[36] J. Goldstone and R. L. Jaffe, Phys. Rev. B **45**, 14100 (1992).

[37] D. C. E. Bortolotti and J. L. Bohn, Phys. Rev. A **69**, 033607 (2004).

[38] A. Szafer and A. D. Stone, Phys. Rev. Lett. **62**, 300 (1989).